Optical Coherence Tomography Detects a Narrowing of the Anterior Chamber Angle in Keratoconus

John O'Neill, MD,[1] Adam Moss, MD, MBA,[1] Michael Page, MD, MA,[1]
George Wandling MD,[1] Alessandro Meduri, MD,[2] Stephen Kaufman, MD, PhD[1,3]

Keratoconus is a bilateral ectatic corneal disorder characterized by progressive corneal thinning and conical protrusion producing irregular astigmatism.[1, 2] Early in the disease course the cornea can appear normal, and recognition of keratoconic changes is made based on a variety of modalities including biomicroscopy, keratometry, pachymetry, and corneal topography. The current standard for diagnosis is through use of Placido disc based topography or scheimpflug imaging, though each has its inherent limitations. [3-10]

Identification of keratoconic corneas is essential to prevent the corneas from entering the eye bank donor pool. Additionally, early diagnosis of the disease is crucial for patients considering LASIK or other refractive procedures. The emergence of collagen crosslinking as a therapeutic modality for keratoconus has further underscored the importance of early detection. Collagen crosslinking uses ultraviolet light and riboflavin to strengthen and stabilize corneal collagen; however it is most effective early in the disease course, highlighting the importance of early diagnosis;.[11] Corneal crosslinking has shown promising results in the short term[11, 12], and long term outcomes have shown stabilization in keratoconus patients out to 10 years.[13] Patients with keratoconus carry a 10-20% lifetime risk of needing a corneal transplant.[14, 15]

Given the prevalence of keratoconus and shortcomings of current diagnostic modalities, it is important to identify cornea donors with keratoconus so that they do not enter the eye bank tissue supply. Thus, it is important to better characterize the disease and to seek out alternate methods to aid in early detection. Newer 3-dimensional imaging systems are now being utilized to evaluate keratoconic changes; including scanning-slit tomography, rotating Scheimpflug imaging, and anterior segment optical coherence tomography (AS-OCT).[16-20]

There have been several studies evaluating AS-OCT to track keratoconic changes. High-speed AS-OCT provides 16 high-resolution (18 μm) cross-sectional images of the anterior segment. Its scanning beam utilizes infrared 1310nm wavelength and obtains 2000 A-scans/sec, thus providing greater penetration and clearer imaging in opaque tissues compared to alternative modalities.[21-23] However, data on the anterior chamber parameters in these eyes with regards to early diagnosis and disease progression in keratoconus is still limited.[16, 18, 24-26] Anterior segment OCT has shown to have good repeatability and reproducibility with regards to measurement of anterior segment angle measurements, with continued improvement as technology evolves.[10, 18, 21, 27-34]

The purpose of our study is to evaluate changes in anterior chamber dimensions in patients with keratoconus using AS-OCT.

METHODS

Subjects

Twenty eyes of 12 patients with keratoconus (5 male and 7 female) and 20 eyes of 10 normal control subjects (3 males and 7 females) were enrolled for this cross-sectional observational study at the University of Minnesota Department of Ophthalmology and Visual Neurosciences, Minneapolis, MN. This study followed the tenants of the Declaration of Helsinki, was in accord with the Health Insurance Portability and Accountability Act of 1996, and was approved by the Institutional Review Board of the University of Minnesota. Written informed consent was obtained from all the subjects. Keratoconic eyes included in this study were diagnosed clinically. All eyes were phakic and had central or paracentral corneal steepening shown on topography. In

Author Affiliation: [1]University of Minnesota, Dept of Ophthalmology, Minneapolis, MN, [2]University of Messina, Dept of Ophthlamology, Messina, Italy [3] Medical College of Wisconsin, Dept of Ophthalmology, Milwaukee, WI

addition, all eyes had at least one clinical sign including slit lamp findings of stromal thinning, anterior conicity, Vogt striae, Fleischer ring, breaks in Descemet's membrane, apical scars, or subepithelial fibrosis. No eyes included in the study had signs or known history of other cornea disease or corneal scarring, and none had undergone previous ocular surgery.

Anterior Segment-Optical Coherence Tomography and Corneal Topography Imaging

Spectral domain AS-OCT scans were acquired with high-resolution (18um) Visante anterior segment OCT (Carl Zeiss Meditec, Inc.). Spectral domain AS-OCT was performed on all study eyes to produce cross sectional images. (Each eye was scanned and the pachymetry maps were calculated and divided into zones by quadrants as previously described.[16] Quadrant values were averaged in the 2-5mm diameter zone. All images were taken by 1 of 3 highly experienced ophthalmic photographers. Placido disc based corneal topography was also performed on all study eyes with either Nidek (Nidek, Freemont, CA) or Atlas (Carl Zeiss Meditec, Inc.) topograph systems. All subjects were undilated, with images obtained in same room under similar lighting conditions. Poor quality images were excluded.

Anterior Segment-Optical Coherence Tomography Parameters

We measured several diagnostic parameters from the AS-OCT imaging, including the trabecular-iris angle (TIA), angle-opening distance at 500 µm (AOD_{500}), anterior chamber depth (ACD), and angle-to-angle distance (ATA), reflecting a previously published method (Figure 1).[27] The average thickness of the superior (S) quadrant minus that of the inferior (I) quadrant (S-I) was calculated from the central 5mm diameter of the pachymetry map with the goal of capturing the asymmetric nature of keratoconic corneal thinning as has been previously demonstrated.[16] All measurements were taken by a single investigator (AM), who was blinded to the patients' group.

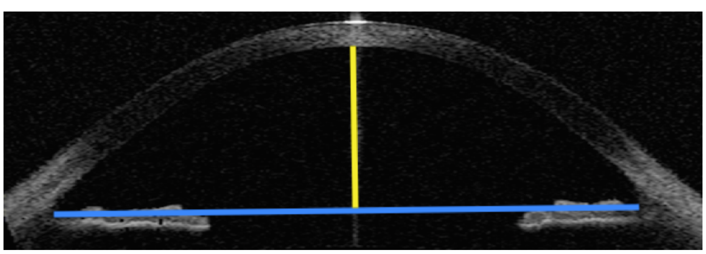

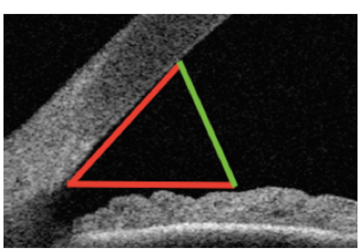

__Figure 1:__ OCT images obtained showing quantitative anterior chamber angle (ACA) parameters. (A) Anterior chamber depth (ACD)(yellow line) and angle-to-angle distance (ATA)(blue line). (B) Angle-opening distance at 500 µm (AOD500)(green line) and trabecular-iris angle (TIA)(red line).

Statistical Analysis – Data were analyzed on an Excel spreadsheet (Microsoft Corp, Redmond, WA). Comparative analysis of visual acuity was performed by converting Snellen acuity to logarithm of the minimum angle of resolution (LogMAR). Statistical comparisons were made using SPSS 19.0 software (IBM Corporation, Armonk, NY). A P value of <0.05 was considered statistically significant.

RESULTS

Keratoconus patients were comprised of 5 males and 12 females, the control group was comprised of 3 males and 10 females. The mean ± standard deviation (SD) age was 44.0 ± 15.7 years in the keratoconus group and 36.2 ± 10.9 years in the control group (p=0.07). The mean spherical equivalent refractive error in this group was -2.32 ± 3.38 in the keratoconus group and -2.82 ± 3.04 in the control group (p=0.63). LogMAR best corrected visual acuity (BCVA) was 0.18 ± 0.28 in the keratoconus group and 0.00 ± 0.02 in the control group (p=0.01) (Table 1).

Anterior chamber angle (ACA) parameters of normal ACA are described in Table 2. Central corneal thickness (CCT)

***Table 1.** Demographic data, refractive error and visual acuities in control and keratoconus groups.*

	Controls (n=20)	**KCN (n=20)**	**P value**
Gender (% Male)	3/10 (30%)	5/12 (42%)	0.74
Age	36.2 ± 10.9	44.0 ± 15.7	0.07
Spherical Equivalent Refractive Error (Diopters)	-2.82 ± 3.04	-2.32 ± 3.38	0.63
BCVA (LogMAR)	0.00 ± 0.02	0.18 ± 0.28	0.01

BCVA= best corrected visual acuity

Table 2. *Corneal thickness and anterior chamber measurements in control and keratoconus groups.*

	Control	**KCN**	**P Value**
aCCT (µm)	539.5 ± 31.9	475.0 ± 58.6	0.0003
ACD (mm)	3.35 ± 0.22	3.53 ± 0.33	0.049
Pupil Diameter (mm)	5.02 ± 1.11	5.08 ± 1.26	0.87
ATA (mm)	12.16 ± 0.53	12.37 ± 0.57	0.23

CCT= central corneal thickness
ACD= anterior chamber depth
ATA= angle-to-angle distance

was significantly thinner in keratoconus patients compared to control (475.0 ± 58.6µm vs 539.5 ± 31.9µm, p=0.0003). ACD was found to be larger in keratoconus patients compared to controls (3.53±0.33 vs 3.35±0.22, p=0.049). There was no significant difference in either pupil diameter or ATA between the groups (Table 2).

The results of the comparison of ACA diagnostic parameters between keratoconus and control eyes is summarized in Table 3. The average TIA measured at the temporal angle was found to be significantly narrowed in keratoconus patients compared to controls (34.74 ± 7.55 degrees vs 40.37

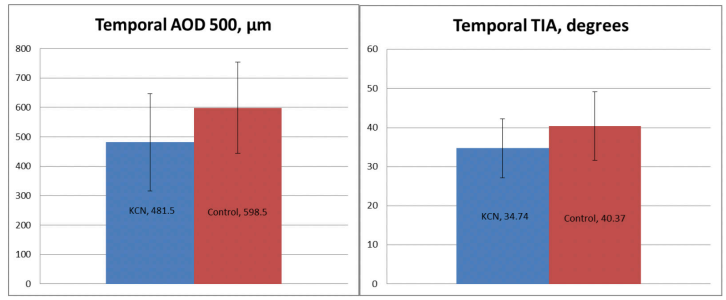

Figure 2. *The average angle-opening distance at 500 µm (AOD500) measured at the temporal angle (left) and average trabecular-iris-angle (TIA) measured at the temporal angle (right) as determined by AS-OCT.*

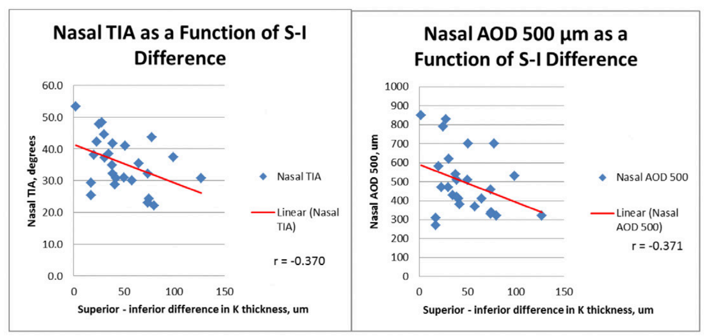

Figure 3. *Correlation coefficient between nasal TIA as a function of average thickness of the superior (S) quadrant minus that of the inferior (I) quadrant (S-I) difference (left) and nasal AOD500 as a function of S-I difference (right).*

Table 3. *Characteristics of the transplanted patients*

	N	Age, years (mean ± SD)	Male, n (%)	Right eye, n (%)	Surgical indication, n (%)	Keratoplasty procedures	Follow-up, months (mean ± SD)	Transplant outcome, n (%)
With diabetic donor	11	61.4 ± 23.5	7 (63.6)	6 (54.5)	BK: 3 (27.3) FED: 1 (9.1) KC: 3 (27.3) Corneal opacity: 2 (18.2) PPD: 1 (9.1) Tectonic: 1 (9.1)	DALK: 2 (18.2) DMEK: 1 (9.1) PK: 8 (72.7)	16.6 ± 6.7	Overall graft success: 9 (81.8) “High risk” graft failure: 2 (18.2)
With non-diabetic donor	48	46.4 ± 21.9	25 (55.6)	24 (53.3)	BK: 5 (10.4) FED: 6 (12.5) Corneal opacity: 10 (20.8) KC: 16 (33.3) Peter’s anomaly: 1 (2.1) PRSE: 1 (2.1) Salzmann: 1 (2.1) Tectonic: 7 (14.6) Therapeutic: 1 (2.1)	DALK: 12 (25) DMEK: 3 (6.3) PK: 33 (68.8)	17.3 ± 6.3	Overall graft success: 39 (81.3) “High risk” graft failure: 2 (4.17) Endothelial rejection: 7 (14.6)
P-value of comparison	-	0.05	0.63	0.94	-	-	0.75	0.97

BK, bullous keratopathy; DALK, deep anterior lamellar keratoplasty; DMEK, Descemet membrane endothelial keratoplasty; FED, Fuchs endothelial dystrophy; KC, keratoconus; PK, penetrant keratoplasty; PPD, posterior polymorphous dystrophy; PRSE, post refractive surgery ectasia; SD, standard deviation.

± 8.76 degrees, p=0.036)(Figure 2). The average AOD_{500} measured at the temporal angle was found to be significantly smaller in keratoconus patients compared to controls (481.5 ± 165.2μm vs 598.5 ± 155.2μm, p=0.027). The TIA and AOD_{500} assessed at the nasal angle also showed a similar trend of narrowing of the anterior chamber angle but did not reach statistical significance.

Figure 3 illustrates the correlation coefficient between nasal AOD_{500} as a function of S-I difference (r=-0.371) and nasal TIA as a function of S-I difference (r=-0.370), demonstrating a linear relationship between nasal ACA flattening as S-I difference increases.

DISCUSSION

In this study, we utilized AS-OCT to evaluate anterior segment parameters in keratoconic patients. It has previously been established that keratoconus is associated with narrowing of the ACA.[10, 26, 27, 33] Our results demonstrate that AS-OCT may be a useful additional tool to screen for keratoconus and for the early detection of keratoconus, monitoring of disease progression, and for improved understanding of the disease biomechanics and pathophysiology.

In 2007 Emre *et al.* used the Pentacam Scheimpflug camera to show progressive narrowing of the ACA in keratoconus with disease progression.[26] McMahon *et al.* also evaluated this phenomenon of peripheral narrowing. Utilizing computer-analyzed, digitized videokeratoscopy they showed a well-defined zone of interior to inferotemporal steepening. These patients had significant flattening away from the cone, particularly in the superonasal quadrant.[35] Our findings support previous observations of peripheral angle narrowing. There was statistically significant narrowing of the temporal ACA, AOD_{500} and TIA in keratoconus patients. The nasal angle measurements also showed peripheral narrowing in the keratoconus patients compared to normal controls, though did not reach statistical significance.

The proposed method of peripheral flattening is a result of biomechanical coupling based on the principle of Gauss's law of elastic domes. It has been shown that surface area is preserved despite curvature changes, thus as curvature increases in the central region of the cone, biomechanical coupling compensates with peripheral flattening.[36] This is analogous to the process by which astigmatic keratotomy produces flattening along the steep meridian to correct for astigmatism. This theory assumes that the cornea behaves as a linear elastic and nearly incompressible material with 3-dimensional orthotropic mechanical properties.

This relationship can be illustrated by Laplace's formula: S=IOP (r/2t), where S is the stress tension on the cornea, IOP is the intraocular pressure, t is the corneal thickness and r is the radius of curvature.[36-38] This formula shows that the central cone in keratoconus with decreased thickness and decreased radius-of-curvature will act as a stress-reducing mechanism to counteract the effect of central thinning. Similarly, in areas of peripheral flattening (areas of increased corneal thickness) there is an increase in the radius-of-curvature, which will allow high stresses to be tolerated without an increase in surface area from stress induced stretching.

The use of central corneal thickness as a measure for evaluating keratoconus has been well established. Numerous studies have established significant thinning in keratoconus as compared to normal corneas.[2, 25, 39-42] In addition to focal thinning, Li *et al.* found that asymmetric and eccentric corneal thinning is also characteristic of keratoconus, particularly when comparing the interior and superior pachymetry measurements using OCT in the central 5mm area of the cornea.[16] We feel the linear relationship shown in Figure 3 comparing the S-I pachymetry maps to nasal ACA measurements AOD_{500} and TIA demonstrates the complementary utility of OCT pachymetry maps and AS-OCT parameters in detection of keratoconus.

Our study was limited by small sample size, inability to control for axial length, and subjectivity involved in making manual ACA measurements. However, in 2011 Liu *et al.* evaluated reliability of AS-OCT and found a high degree of reproducibility for angle measurements as shown by both intra and inter-observer reproducibility coefficients and intra-class correlation coefficients.[32] Reproducibility of ACA measurements by AS-OCT has also been demonstrated with inter-session and inter-operator agreement for temporal AOD_{500}.[27] We feel that AS-OCT has been shown to produce consistent anterior chamber angle measurements, and is thus a reliable metric for evaluation of early keratoconic changes.

In the present study, we only assessed nasal and temporal anterior chamber angles. Further evaluation of superior and inferior angle structures given the pachymetric relationship in these areas for early detection of keratoconus may provide increased sensitivity and specificity in disease detection. Despite the demonstrated reliability of AS-OCT ACA measurements, automated software to validate current data with the goal of decreased subjectivity, improved reproducibility and additional measurements would further improve this imaging modality. Finally, long term prospective monitoring of disease progression with repeated imaging will further validate AS-OCT as a measure for early detection.

CONCLUSION

AS-OCT has been shown to be a valid and reliable diagnostic tool to identify keratoconus. This is particularly important to prevent ectatic corneal tissue, from keratoconus, from entering the eye bank tissue supply, and given the increasing emphasis on early detection in light of new treatment modalities such as corneal crosslinking. Our study suggests that keratoconus produces a central corneal steepening and a peripheral corneal flattening associated with narrowing of the anterior chamber angle. These findings may be useful as an alternate method for keratoconus detection and monitoring of disease progression, and may provide a better understanding of the pathophysiology of keratoconus

REFERENCES

1. Krachmer JH, Feder RS, Belin MW. Keratoconus and related noninflammatory corneal thinning disorders. *Surv Ophthalmol.* Jan-Feb 1984;28(4):293-322.
2. Rabinowitz YS. Keratoconus. *Surv Ophthalmol.* Jan-Feb 1998;42(4):297-319.
3. Avitabile T, Franco L, Ortisi E, et al. Keratoconus staging: a computer-assisted ultrabiomicroscopic method compared with videokeratographic analysis. *Cornea.* Oct 2004;23(7):655-660.
4. Li X, Rabinowitz YS, Rasheed K, Yang H. Longitudinal study of the normal eyes in unilateral keratoconus patients. *Ophthalmology.* Mar 2004;111(3):440-446.
5. Maguire LJ, Bourne WM. Corneal topography of early keratoconus. *Am J Ophthalmol.* Aug 15 1989;108(2):107-112.
6. Rabinowitz YS, Garbus J, McDonnell PJ. Computer-assisted corneal topography in family members of patients with keratoconus. *Arch Ophthalmol.* Mar 1990;108(3):365-371.
7. Wilson SE, Lin DT, Klyce SD. Corneal topography of keratoconus. *Cornea.* Jan 1991;10(1):2-8.
8. Wilson SE, Lin DT, Klyce SD, Reidy JJ, Insler MS. Topographic changes in contact lens-induced corneal warpage. *Ophthalmology.* Jun 1990;97(6):734-744.
9. Maeda N, Klyce SD, Smolek MK. Comparison of methods for detecting keratoconus using videokeratography. *Arch Ophthalmol.* Jul 1995;113(7):870-874.
10. Nakagawa T, Maeda N, Higashiura R, Hori Y, Inoue T, Nishida K. Corneal topographic analysis in patients with keratoconus using 3-dimensional anterior segment optical coherence tomography. *J Cataract Refract Surg.* Oct 2011;37(10):1871-1878.
11. Wollensak G. Crosslinking treatment of progressive keratoconus: new hope. *Curr Opin Ophthalmol.* Aug 2006;17(4):356-360.
12. Vinciguerra P, Albe E, Trazza S, et al. Refractive, topographic, tomographic, and aberrometric analysis of keratoconic eyes undergoing corneal cross-linking. *Ophthalmology.* Mar 2009;116(3):369-378.
13. Raiskup F, Theuring A, Pillunat LE, Spoerl E. Corneal collagen crosslinking with riboflavin and ultraviolet-A light in progressive keratoconus: ten-year results. *J Cataract Refract Surg.* Jan 2015;41(1):41-46.
14. Rabinowitz YS, Rasheed K, Yang H, Elashoff J. Accuracy of ultrasonic pachymetry and videokeratography in detecting keratoconus. *J Cataract Refract Surg.* Feb 1998;24(2):196-201.
15. Tuft SJ, Moodaley LC, Gregory WM, Davison CR, Buckley RJ. Prognostic factors for the progression of keratoconus. *Ophthalmology.* Mar 1994;101(3):439-447.
16. Li Y, Meisler DM, Tang M, et al. Keratoconus diagnosis with optical coherence tomography pachymetry mapping. *Ophthalmology.* Dec 2008;115(12):2159-2166.
17. Doors M, Berendschot TT, de Brabander J, Webers CA, Nuijts RM. Value of optical coherence tomography for anterior segment surgery. *J Cataract Refract Surg.* Jul 2010;36(7):1213-1229.
18. Ramos JL, Li Y, Huang D. Clinical and research applications of anterior segment optical coherence tomography - a review. *Clin Experiment Ophthalmol.* Jan 2009;37(1):81-89.
19. Belin MW, Khachikian SS. An introduction to understanding elevation-based topography: how elevation data are displayed - a review. *Clin Experiment Ophthalmol.* Jan 2009;37(1):14-29.
20. Cairns G, McGhee CN. Orbscan computerized topography: attributes, applications, and limitations. *J Cataract Refract Surg.* Jan 2005;31(1):205-220.
21. Leung CK, Weinreb RN. Anterior chamber angle imaging with optical coherence tomography. *Eye (Lond).* Mar 2011;25(3):261-267.
22. Memarzadeh F, Li Y, Francis BA, Smith RE, Gutmark J, Huang D. Optical coherence tomography of the anterior segment in secondary glaucoma with corneal opacity after penetrating keratoplasty. *Br J Ophthalmol.* Feb 2007;91(2):189-192.
23. Khurana RN, Li Y, Tang M, Lai MM, Huang D. High-speed optical coherence tomography of corneal opacities. *Ophthalmology.* Jul 2007;114(7):1278-1285.
24. Barkana Y, Gerber Y, Elbaz U, et al. Central corneal thickness measurement with the Pentacam Scheimpflug system, optical low-coherence reflectometry pachymeter, and ultrasound pachymetry. *J Cataract Refract Surg.* Sep 2005;31(9):1729-1735.
25. Gherghel D, Hosking SL, Mantry S, Banerjee S, Naroo SA, Shah S. Corneal pachymetry in normal and keratoconic eyes: Orbscan II versus ultrasound. *J Cataract Refract Surg.* Jun 2004;30(6):1272-1277.
26. Emre S, Doganay S, Yologlu S. Evaluation of anterior segment parameters in keratoconic eyes measured with the Pentacam system. *J Cataract Refract Surg.* Oct 2007;33(10):1708-1712.
27. Kim DY, Sung KR, Kang SY, et al. Characteristics and reproducibility of anterior chamber angle assessment by anterior-segment optical coherence tomography. *Acta Ophthalmol.* Aug 2011;89(5):435-441.
28. Goldsmith JA, Li Y, Chalita MR, et al. Anterior chamber width measurement by high-speed optical coherence tomography. *Ophthalmology.* Feb 2005;112(2):238-244.
29. Muller M, Dahmen G, Porksen E, et al. Anterior chamber angle measurement with optical coherence tomography: intraobserver and interobserver variability. *J Cataract Refract Surg.* Nov 2006;32(11):1803-1808.
30. Leung CK, Palmiero PM, Weinreb RN, et al. Comparisons of anterior segment biometry between Chinese and Caucasians using anterior segment optical coherence tomography. *Br J Ophthalmol.* Sep 2010;94(9):1184-1189.
31. Cheung CY, Zheng C, Ho CL, et al. Novel anterior-chamber angle measurements by high-definition optical coherence tomography using the Schwalbe line as the landmark. *Br J Ophthalmol.* Jul 2011;95(7):955-959.
32. Liu S, Yu M, Ye C, Lam DS, Leung CK. Anterior chamber angle imaging with swept-source optical coherence tomography: an investigation on variability of angle measurement. *Invest Ophthalmol Vis Sci.* 2011;52(12):8598-8603.
33. Szalai E, Berta A, Hassan Z, Modis L, Jr. Reliability and repeatability of swept-source Fourier-domain optical coherence tomography and Scheimpflug imaging in keratoconus. *J Cataract Refract Surg.* Mar 2012;38(3):485-494.
34. Tian J, Marziliano P, Baskaran M, Wong HT, Aung T. Automatic anterior chamber angle assessment for HD-OCT images. *IEEE Trans Biomed Eng.* Nov 2011;58(11):3242-3249.

35. McMahon TT, Robin JB, Scarpulla KM, Putz JL. The spectrum of topography found in keratoconus. *CLAO J.* Jul 1991;17(3):198-204.

36. Smolek MK, Klyce SD. Is keratoconus a true ectasia? An evaluation of corneal surface area. *Arch Ophthalmol.* Sep 2000;118(9):1179-1186.

37. Perkins E. Myopia and Scleral Stress. *Doc Ophthalmol Proc Series.* 1981;28:121-127.

38. Poole TA. Calculation of stress distribution in keratoconus. *N Y State J Med.* Jun 1 1973;73(11):1284-1288.

39. Pflugfelder SC, Liu Z, Feuer W, Verm A. Corneal thickness indices discriminate between keratoconus and contact lens-induced corneal thinning. *Ophthalmology.* Dec 2002;109(12):2336-2341.

40. Ambrosio R, Jr., Alonso RS, Luz A, Coca Velarde LG. Corneal-thickness spatial profile and corneal-volume distribution: tomographic indices to detect keratoconus. *J Cataract Refract Surg.* Nov 2006;32(11):1851-1859.

41. Lim L, Wei RH, Chan WK, Tan DT. Evaluation of keratoconus in Asians: role of Orbscan II and Tomey TMS-2 corneal topography. *Am J Ophthalmol.* Mar 2007;143(3):390-400.

42. Ucakhan OO, Ozkan M, Kanpolat A. Corneal thickness measurements in normal and keratoconic eyes: Pentacam comprehensive eye scanner versus noncontact specular microscopy and ultrasound pachymetry. *J Cataract Refract Surg.* Jun 2006;32(6):970-977.

43. Tang M, Shekhar R, Miranda D, Huang D. Characteristics of keratoconus and pellucid marginal degeneration in mean curvature maps. *Am J Ophthalmol.* Dec 2005;140(6):993-1001.

